A class of selective antibacterials derived from a protein kinase inhibitor pharmacophore

J. Richard Miller[a,1,2,3], Steve Dunham[a,1,4], Igor Mochalkin[a,1,2], Craig Banotai[a], Matthew Bowman[a], Susan Buist[a], Bill Dunkle[a,4], Debra Hanna[a,2], H. James Harwood[b], Michael D. Huband[a,2], Alla Karnovsky[a], Michael Kuhn[a,2], Chris Limberakis[a,2], Jia Y. Liu[a], Shawn Mehrens[a,2], W. Thomas Mueller[a,5], Lakshmi Narasimhan[a,6], Adam Ogden[a,2], Jeff Ohren[a,b], J. V. N. Vara Prasad[a], John A. Shelly[a,4], Laura Skerlos[a], Mark Sulavik[a], V. Hayden Thomas[a,2], Steve VanderRoest[a], LiAnn Wang[c], Zhigang Wang[a,7], Amy Whitton[a], Tong Zhu[a,2], and C. Kendall Stover[a,4]

[a]Pfizer, Inc., Ann Arbor, MI 48105; [b]Pfizer, Inc., Groton, CT 06340; and [c]Pfizer, Inc., Cambridge, MA 02139

Edited by Michael A. Marletta, University of California, Berkeley, CA, and approved December 5, 2008 (received for review November 10, 2008)

As the need for novel antibiotic classes to combat bacterial drug resistance increases, the paucity of leads resulting from target-based antibacterial screening of pharmaceutical compound libraries is of major concern. One explanation for this lack of success is that antibacterial screening efforts have not leveraged the eukaryotic bias resulting from more extensive chemistry efforts targeting eukaryotic gene families such as G protein-coupled receptors and protein kinases. Consistent with a focus on antibacterial target space resembling these eukaryotic targets, we used whole-cell screening to identify a series of antibacterial pyridopyrimidines derived from a protein kinase inhibitor pharmacophore. In bacteria, the pyridopyrimidines target the ATP-binding site of biotin carboxylase (BC), which catalyzes the first enzymatic step of fatty acid biosynthesis. These inhibitors are effective in vitro and in vivo against fastidious Gram-negative pathogens including *Haemophilus influenzae*. Although the BC active site has architectural similarity to those of eukaryotic protein kinases, inhibitor binding to the BC ATP-binding site is distinct from the protein kinase-binding mode, such that the inhibitors are selective for bacterial BC. In summary, we have discovered a promising class of potent antibacterials with a previously undescribed mechanism of action. In consideration of the eukaryotic bias of pharmaceutical libraries, our findings also suggest that pursuit of a novel inhibitor leads for antibacterial targets with active-site structural similarity to known human targets will likely be more fruitful than the traditional focus on unique bacterial target space, particularly when structure-based and computational methodologies are applied to ensure bacterial selectivity.

acetylcoenzyme A carboxylase | biotin carboxylase | crystal structure | high-throughput screening | fatty acid biosynthesis

The well-documented increase in antibacterial resistance over the past few decades has led to intensive efforts to discover novel antibacterial agents. Literally thousands of new essential bacterial targets from human pathogens were identified as a result of the genomics revolution (1–3). This necessitated a means to "triage" these targets to identify the most promising ones to pursue by high throughput screening of pharmaceutical compound files. In these target analyses, one desirable attribute was little or no sequence and/or structural homology to human gene products to improve the chances of finding bacterial-selective hits. However, this selection criterion could also have a deleterious effect on the number of potent hits identified because the medicinal chemistry efforts that built these compound files were largely focused on human therapeutic targets such as kinases, G protein-coupled receptors, proteases, etc. (1–4). Therefore, pursuit of bacterial targets with the greatest sequence and/or structural relatedness to proven eukaryotic drug targets could be more fruitful. Consistent with this hypothesis, we used unbiased whole-bacterial cell screening of the Pfizer compound library to discover a series of antibacterial pyridopyrimidines (**1**, **2**, and **3**; Fig. 1*A*) that emerged from a structure-based drug design program targeting eukaryotic tyrosine protein kinases (5). By using genetic and biochemical tools, the bacterial target of these compounds was identified as biotin carboxylase (BC); one portion of the acetyl-CoA carboxylase (ACCase) multienzyme complex responsible for the first step of fatty acid biosynthesis (6). BC has an active site with considerable structural similarity to eukaryotic protein kinases, yet it is sufficiently different to allow for selectivity against both human kinases and the eukaryotic ACCase.

The identification of selective antibacterials containing a kinase inhibitor pharmacophore has intriguing implications for antibacterial drug discovery, particularly given that the targets, biotin carboxylase and eukaryotic protein kinases, have structurally related ATP-binding sites. It remains to be seen if the huge array of eukaryotic inhibitors present in pharmaceutical libraries can be mined for their activity against structurally related bacterial targets such as the bacterial histidine kinases involved in cell–cell signaling, lipopolysaccharide sugar kinases involved in Gram-negative cell wall formation, antibiotic kinases that deactivate specific antibacterial agents, or less obvious targets, such as biotin carboxylase. Our results argue that there may be value in reassessing antibacterial target space for previously unexplored (or underexplored) targets amenable to an approach based on repurposing eukaryotic pharmacophores.

Results

Identification of Antibacterial Pyridopyrimidines. As part of our antibacterial drug discovery effort, a library of ≈1.6 million

Author contributions: J.R.M., S.D., I.M., S.B., D.H., L.N., A.O., J.V.N.V.P., M.S., V.H.T., Z.W., T.Z., and C.K.S. designed research; J.R.M., S.D., I.M., C.B., M.B., S.B., B.D., M.D.H., M.K., C.L., J.Y.L., S.M., W.T.M., L.N., A.O., J.O., J.V.N.V.P., J.A.S., L.S., S.V., L.W., Z.W., and A.W. performed research; J.R.M., S.D., I.M., C.B., M.B., B.D., H.J.H., A.K., M.K., C.L., J.Y.L., S.M., W.T.M., L.N., J.V.N.V.P., J.A.S., V.H.T., S.V., and Z.W. contributed new reagents/analytic tools; J.R.M., S.D., I.M., M.B., S.B., D.H., H.J.H., M.D.H., A.K., C.L., J.Y.L., L.N., A.O., J.O., J.V.N.V.P., L.S., M.S., L.W., Z.W., A.W., T.Z., and C.K.S. analyzed data; and J.R.M., S.D., I.M., J.O., and C.K.S. wrote the paper.

The authors declare no conflict of interest.

This article is a PNAS Direct Submission.

Data deposition: The atomic coordinates and structure factors have been deposited in the Protein Data Bank, www.pdb.org [PDB IC codes 2V58 (compound **1**), 2V59 (compound **2**), and 2V5A (compound **3**)].

See Commentary on page 1689.

[1]J.R.M., S.D., and I.M. contributed equally to this work.

[2]Present address: Pfizer, Inc., Groton, CT 06340.

[3]To whom correspondence should be addressed at the present address: Pfizer, Inc., Eastern Point Road, Groton, CT 06340. E-mail: richard.miller2@pfizer.com.

[4]Present address: Pfizer, Inc., Kalamazoo, MI 49007.

[5]Present address: Pfizer, Inc., Chesterfield, MO 63017.

[6]Present address: Pfizer, Inc., La Jolla, CA 92121.

[7]Present address: Pfizer, Inc., Cambridge, MA 02139.

This article contains supporting information online at www.pnas.org/cgi/content/full/0811275106/DCSupplemental.

© 2009 by The National Academy of Sciences of the USA

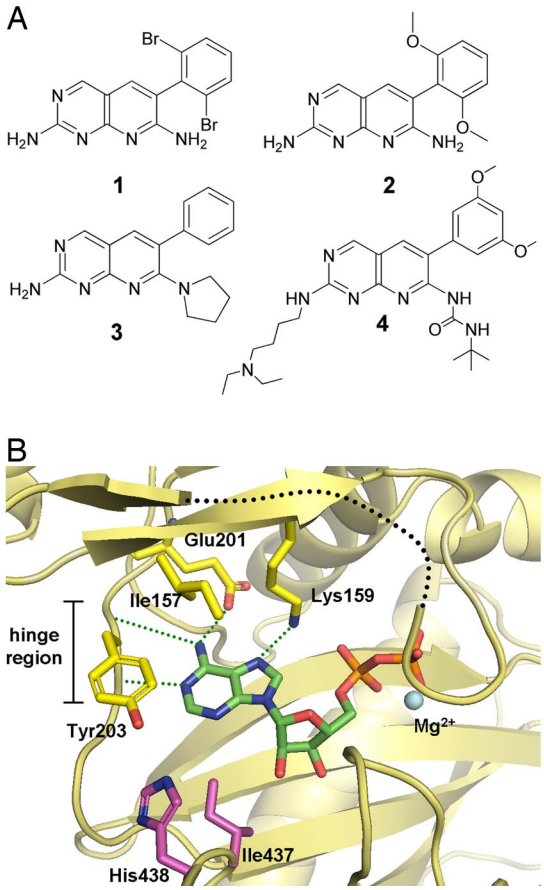

Fig. 1. Pyridopyrimidine inhibitor structures and sites of resistance-conferring mutations in biotin carboxylase. (*A*) Pyridopyrimidine inhibitors of BC (**1**, **2**, and **3**) and FGFR1 (**4**). (*B*) X-ray costructure of ADP and *E. coli* BC (8). Residues conferring resistance to **1** upon mutation are highlighted.

individual compounds was screened for growth inhibition of a membrane-compromised, efflux pump-deficient strain of *Escherichia coli* (*tolC*, *imp*). The pyridopyrimidines, typified by **1**, **2**, and **3**, were among the inhibitors identified in this screen. These compounds exhibit potent antibacterial activity against the screening strain and several other human pathogens (Table 1). Most notable was their exquisite potency against clinical isolates of fastidious Gram-negative pathogens such as *Haemophilus influenzae* and *Moraxella catarrhalis*; causative agents of many respiratory tract infections. Identification of these compounds as antibacterials was intriguing given their pharmaceutical history. N2-substituted analogs (typified by **4**) are potent inhibitors of the VEGFR2 and FGFR1 eukaryotic protein kinases (Table 3) (5). In the pretarget-based drug discovery era of the 1970s–1980s, members of this series were also investigated as potassium-sparing diuretics with antihypertensive effects in rats (7).

Mechanism of Pyridopyrimidine Antibacterial Activity. To determine whether the antibacterial activity of **1** and **2** was caused by a specific mechanism of action, a biological macromolecular biosynthesis assay was used. Compounds **1** and **2** specifically inhibit fatty acid biosynthesis in *E. coli* (Table 2). Spontaneous mutations conferring resistance to at least 8 times the minimal inhibitory concentration (MIC) of **1** were isolated at frequencies of ≈1 in 10^9 in *E. coli*, *H. influenzae*, and *M. catarrhalis* [supporting information (SI) Tables S1 and S2]. The mutations responsible for resistance were mapped and confirmed by backcross experiments to the *accC* gene, which encodes the BC component of ACCase. ACCase utilizes ATP,

Table 1. Microbiological data for BC inhibitors: MIC and MBC in μg mL^{-1}

Strain (genotype)*	Compound tested				
Additives	**1**	**1**	**2**	**3**	Linezolid
Test type	MIC	MBC	MIC	MIC	MIC
E. coli (*tolC*, *imp*−)	0.125	1	2	8	8
E. coli (*tolC*, *imp*−), 2% HSA†	0.5		4	32	8
E. coli (wild type)	16	32	>64	>64	>64
H. influenzae (*acrA*)	0.125		0.5	4	8
H. influenzae (wild type)	0.125	0.5	1	32	16
H. influenzae (*accC*-I437T)	16	32	64	>64	8
M. catarrhalis (*acrA*)	0.5		2	8	8
M. catarrhalis (wild type)	1	2	2	8	8
S. aureus (*norA*)	16		32	64	2
S. aureus (MRSA)	32	64	>64	>64	2
S. pneumoniae (wild type)‡	>64		>64	>64	2
E. faecalis (wild type)§	>64		>64	>64	2
P. aeruginosa (*mexAB oprM*)	32		>64	>64	64
P. aeruginosa (wild type)	>64		>64	>64	>64

*The following designate targeted knockouts of efflux pumps or subunits of efflux pumps: *tolC*, *acrA*, *norA*, *mexAB*, and *oprM*. The *imp* gene disruption further sensitizes *E. coli* to inhibitors. The *accC*-I437T genotype in *Haemophilus* results from spontaneously resistant mutants selected in the presence of compound **1**.
†Human serum albumin.
‡*Streptococcus pneumoniae*.
§*Enterococcus faecalis*.

bicarbonate, and acetyl-CoA to catalyze formation of malonyl-CoA (Fig. S1) and is the first committed step in fatty acid biosynthesis (6). When the *H. influenzae* resistance-conferring mutations were mapped onto the crystal structure of *E. coli* BC containing bound ADP (8), the mutations clustered within the ATP-binding pocket (Fig. 1*B* and Table S2), indicating that the pyridopyrimidines likely interact with this portion of the BC active site. This finding is consistent with prior knowledge that members of this chemical class bind the ATP site of FGFR kinase (9) and are competitive with ATP (5, 10).

Pyridopyrimidines Bind Bacterial BC. Molecular interaction of **1** with purified BC from *E. coli*, *H. influenzae*, *Pseudomonas aeruginosa*, and *Saccharomyces aureus* was confirmed by isothermal titration calorimetry (ITC) and/or surface plasmon resonance (SPR, Fig. S2, Table 4, and Table S3). Binding of **1** to *E. coli* BC is enthalpically driven, potent (K_d 800 ± 200 pM) and exhibits a slow dissociation rate from the enzyme. The pyridopyrimidine inhibitors are also potent (Table 3) in an enzyme-coupled *E. coli* ACCase holoenzyme reaction (Fig. S1). Inhibition in this assay, which requires biotinylated biotin carboxyl carrier protein, carboxytransferase, and BC for turnover, demonstrates that pyridopyrimidine binding to BC inhibits the physiologically relevant ACCase holoenzyme reaction.

Purified active BC enzyme from *E. coli*, *H. influenzae*, and *P. aeruginosa* readily crystallized with **1**, **2**, and subsequently with numerous analogs thereof, yielding high-resolution crystal structures to guide structure-based lead optimization. The unambiguous electron density map of inhibitor **1** (Fig. 2*A*) described a consistent binding mode of the pyridopyrimidine inhibitors at the BC ATP-

Table 2. *E. coli* (*tolC imp*) macromolecular synthesis assay IC_{50} (μg mL^{-1})

Pathway	Compound **1**	Triclosan
Cell growth	0.125	0.1
DNA	>50	>10
RNA	>50	>10
Protein	>50	>10
Fatty acid	<1	1.3

Table 3. Biochemistry of BC inhibitors

Assay IC_{50} (nM) at 1× $K_{m(ATP)}$	Compound 1	2	3	4
Enzyme-coupled *E. coli* ACCase				
Wild-type	<5	28	150	>10,000
I437T mutant	560	7,300	2,100	ND*
H438P mutant	160	1,200	1,300	ND
Rat liver ACCase	>100,000	>100,000	ND	ND
FGFR1 kinase	5,800	>30,000	>10,000	17
VEGFR2 kinase	>30,000	>30,000	>10,000	420

*ND, not determined.

Table 4. Biophysics of inhibitor binding to *E. coli* BC

Parameter	Compound 1	Compound 2
k_{on}, $M^{-1}s^{-1}$	(4.90 ± 1.35) × 10^7	(2.36 ± 0.04) × 10^7
k_{off}, s^{-1}	0.041 ± 0.022	0.15 ± 0.01
K_d from SPR, nM	0.82 ± 0.22	6.53 ± 0.64
K_d from ITC, nM	<5.0	18 ± 9
Δ*H*, kcal/mol	−18.0 ± 0.1	−16.47 ± 0.02
ΔG, kcal/mol	<(−11.5)	−10.7
TΔ*S*, kcal/mol	−6.5	−5.8

binding site with the compound engaged in an extensive ligand-efficient network of interactions within the adenine-binding region, whereas the bisubstituted phenyl group occupied the hydrophobic pocket neighboring the ribose-binding site (Fig. 2*B* and Fig. S3). These data provide conclusive linkage of pyridopyrimidine antibacterial activity to inhibition of a unique biosynthetic enzyme target.

Antibacterial Pyridopyrimidines Are Selective for Bacterial BC. The distinctively different binding modes (Fig. 2 *C* and *D*) of pyridopyrimidines observed in the BC and FGFR2 kinase domain crystal structures (9) suggested that BC selectivity could be achieved despite considerable structural similarity of the ATP-binding sites. Indeed, **1** and **2** display excellent selectivity for bacterial BC over FGFR2, VEGFR1, and 28 other eukaryotic protein kinases (Table 3 and Fig. 3). Src was the only eukaryotic protein kinase tested that was significantly inhibited by **1** (however, the Src IC_{50} of compound **1** is still 70-fold weaker than its IC_{50} against *E. coli* BC).

Pyridopyrimidines Are Bactericidal. Further efforts focused on assessment of the potential clinical utility of these compounds. Minimal bactericidal concentrations (MBC) (11, 12) were determined to be 2- to 4-fold higher than MICs for compounds **1**, **2**, and **3,** indicating that these compounds are bactericidal against *E. coli*, *H. influenzae*, *M. catarrhalis*, and *S. aureus* (Table 1). Measurements of the kinetics of bacterial killing confirm that **1** is bactericidal (defined as a >99.9% reduction in viable bacteria within 24 h) (12) against *H. influenzae* within 14 h at ≥2-fold above its MIC (Fig. 4*A*).

Pharmacokinetics of Pyridopyrimidines. The pharmacokinetic properties of **1** were assessed in vitro and in vivo by using rat and mouse (Table 5). At low i.v. doses (5 mg/kg), **1** was rapidly cleared. Total body clearance was greater than liver blood flow in rat and mouse (clearance = 100 and 150 mL per min per kg, respectively). However, at higher oral doses (200 mg/kg), **1** shows >100% bioavailability, likely caused by saturation of rodent clearance mechanisms. The high clearance of **1** observed in rat was predicted by rat liver microsomes. Because human liver microsomes predict dramatically lower clearance in humans, scaling from rodent clearance may overestimate human clearance.

Pyridopyrimidine BC Inhibitors Have in Vivo Antibacterial Activity. Based on the reasonable pharmacokinetic properties of **1**, it was tested in murine models of tissue-localized (thigh) and systemic *H. influenzae* infection. In the thigh model, **1** showed a good correlation between plasma concentrations 24 h after therapy (oral dosing) and reduction of bacterial levels in thigh tissue (Fig. 4*B*). Assuming that 24-h plasma concentrations are representative of total exposures, the 24-h plasma concentration that related to achieving 50% of the maximum effect was 5.6 ± 1.8 μg/mL. Similarly, in a *H. influenzae* murine systemic infection model, oral dosing of animals at 200 mg/kg once or twice a day resulted in 63% and 50% survival, respectively (Table S4). No overt toxicity was observed with **1** at all doses tested in efficacy studies.

Pyridopyrimidines Show Improved in Vitro Antibacterial Activity in Combination with Other Antibacterial Agents. Collectively, these data indicate that our pyridopyrimidine BC inhibitors show promise as clinically useful agents against fastidious Gram-negative organisms. Although a trend toward more selective antibacterial classes may be desirable to combat unintentional selection for antibiotic resistance and take advantage of current and future improvements in molecular diagnostics (13), the acceptance of empiric therapy for fastidious Gram-negative or other single-agent infections would be unlikely in the absence of a rapid, inexpensive, and highly accurate diagnostic (14). Furthermore, the observation of single-step high-level resistance to **1** and **2** could be of concern despite the relatively low frequency of occurrence. Acceptance of a pyridopyrimidine BC inhibitor into empiric clinical use might therefore require demonstration that it could be used in combination with other antibiotics possessing a complimentary spectrum and that resistance development potential can be minimized by using structural and/or computational tools to guide inhibitor design.

To assess whether the combination of BC inhibitors with other antibacterials resulted in improved antibacterial spectrum, we tested **1** along with several other antibacterials in vitro by using a checkerboard susceptibility approach (15). Compound **1** was not antagonistic with any of the tested agents or organisms, including Gram-positive bacteria (Table 6). This finding is important because compound **1** could be useful in combination with Gram-positive antibacterials that lack potent activity against *H. influenzae* and other fastidious Gram-negative pathogens. Combinations showing conclusive synergy with compound **1** were triclosan [fractional inhibitory concentration (FIC) = 0.37] and ciprofloxacin (FIC = 0.26) in *H. influenzae* (Table 6). The observation of triclosan synergy is consistent with the mechanism of action experiments because both triclosan and compound **1** target enzymes involved in fatty acid biosynthesis. This result provides further confirmation of the validity of the fatty acid biosynthesis pathway as a source of potential antimicrobial targets (16, 17).

Use of Structural Biology to Ameliorate Pyridopyrimidine Resistance Development. Low-frequency spontaneous single-step mutations in the *accC* gene (e.g., I437T in *E. coli* BC and others described in Tables S1 and S2) resulted in variable loss of affinity for **1** and **2** and corresponding decreases in antibacterial activity (Tables 1 and 3 and Table S2). The molecular basis for pyridopyrimidine resistance in the I437T *E. coli* mutant was apparent upon examination of the X-ray crystal structure of **1** bound to the I437T mutant (Fig. S4). This costructure revealed that the I437T mutation results in a decrease in shape complementarity between the inhibitor and the binding pocket as well as a loss of hydrophobic contacts between I437 and the substituted phenyl ring. Mining the Pfizer compound file (including compounds not screened in our initial high-throughput screen) for structurally related pyridopyrimidines less affected by the I437T mutation identified compound **3** (*E. coli* BC IC_{50} = 150 nM), which was only 14-fold less active against the I437T BC mutant. Based on the crystal structures, the C7-substituted

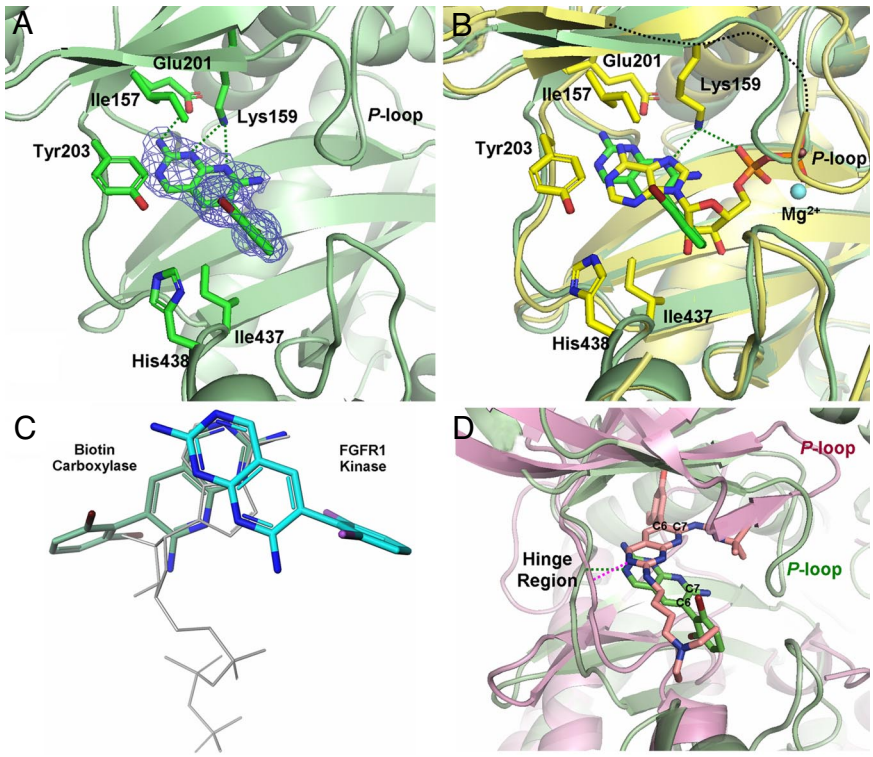

Fig. 2. Binding modes of pyridopyrimidine inhibitors. (*A*) View of the unambiguous ($F_o - F_c$) OMIT electron density map of inhibitor **1** calculated by omitting **1** during simulated annealing. Map is superimposed on the final refined model and contoured at 2.5 σ level. Inhibitor **1** is shown in sticks with the following atom colors: carbon, green; nitrogen, blue; oxygen, red; and bromine, cherry red. Ribbon representation of BC is in green. (*B*) View of the superimposed ATP-binding site in complexes with inhibitor **1** and ADP [Protein Data Bank (PDB) ID code 2j9g]. Ribbon representation of the *Ec*BC/inhibitor **1** coordinates is in green. Ribbon representation of the *Ec*BC/ADP coordinates is in yellow. *Ec*BC residues involved in interactions with ADP are shown in sticks with the following atom colors: carbon, yellow; nitrogen, blue; oxygen, red. (*C*) Overlay of compound **1** bound in the ATP-binding site of BC (green carbons) vs. compound **1** docked into the ATP-binding site of FGFR1 (PDB ID code 2fgi; cyan carbons). The conformation of ATP bound to both kinases is shown in gray as a guide. (*D*) View of the distinctively different binding modes of inhibitor **1** and compound **4** in the superimposed ATP-binding sites of BC and FGFR1 (PDB ID code 2fgi). Ribbon representation of the *Ec*BC/inhibitor **1** coordinates is in green. Ribbon representation of the FGFR/compound **4** coordinates is in pink. Images were prepared by using PyMOL molecular graphics systems (DeLano Scientific LLC).

pyrrolidine group of compound **3** utilizes favorable hydrophobic interactions with the side chain of Ile-287 and the P-loop, partially compensating for the loss of binding affinity. In this respect, the ease of obtaining crystal structures of multiple inhibitor analogs substituted at the C6, C7, or both positions bound to the wild-type and resistant BC enzymes offers the opportunity to use structure-based drug design approaches to circumvent target-based resistance mechanisms and develop structure activity and structure resistance relationships. Furthermore, residue 437 (*E. coli* numbering) represents a key difference in the Gram-negative and Gram-positive BC active site. Gram-negatives have isoleucine at this position and Gram-positives, threonine (Table S5). This suggests that inhibitor design focusing on this residue difference could enhance the Gram-positive antibacterial spectrum of the pyridopyrimidines and alleviate this resistance mechanism in Gram-negative organisms.

Discussion

We report the discovery of a class of potent synthetic antibacterials that have potential as standalone agents targeting fastidious Gram-negative pathogens or as broader spectrum agents when used in combination with existing antibiotics. Although the discovery of a previously undescribed class of antibacterials is in itself significant, we believe the pharmaceutical origins of these inhibitors have far-reaching implications for antibacterial drug discovery in general. The BC inhibitors **1**, **2**, and **3** originated as weakly active analogs from structure-guided eukaryotic drug discovery programs targeting eukaryotic protein kinases. Despite their origin, or, perhaps because of their origin, these inhibitors act on the structurally related ATP-binding site of a previously undescribed bacterial target.

Discovery of these BC inhibitors by whole-cell screening and reverse genetics underscores the utility of this screening approach

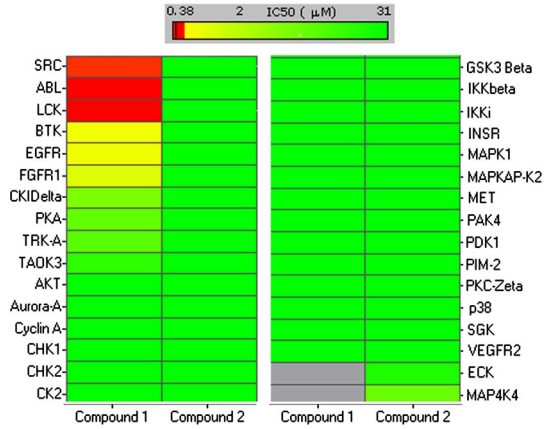

Fig. 3. Heat map representation of the inhibition of several eukaryotic protein kinases by compounds **1** and **2**. (*Upper*) Scale shows relative potencies. The color transition is nonlinear to greater highlight the few kinases that showed weak inhibition by compound **1**. (*Lower*) Kinase assays were performed by using commercially available or in-house generated reagents at the Pfizer Kinase Center of Emphasis, Cambridge, MA.

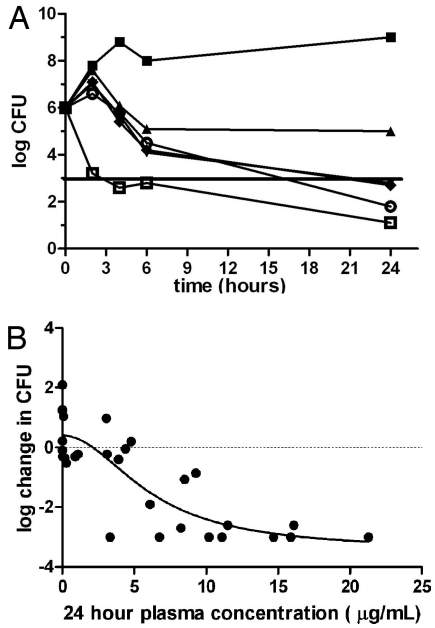

Fig. 4. In vitro and in vivo efficacy of pyridopyrimidines. (*A*) Kinetics of *H. influenzae* killing in vitro by compound **1**. The number of viable *H. influenzae* was determined after treatment with various concentrations of **1** or ciprofloxacin for various times. Filled squares represent the growth control (no inhibitor). Open squares represent treatment with ciprofloxacin (4-fold over MIC). Filled triangles, filled diamonds, open circles, and open squares show treatment with 1-, 2-, 4-, and 8-fold over the MIC of 1, respectively. The solid horizontal line denotes a 3-log reduction in bacteria relative to time 0. (*B*) In vivo efficacy of compound **1** in a murine *H. influenzae* thigh infection. Circles represent the number of recoverable bacteria (*y* axis) from the infected thigh of an individual mouse with a given plasma concentration of **1**, 24 h after dosing (*x* axis). The solid line represents the fit of the data to an inhibitory sigmoid E_{max} model.

and demonstrates the need to reassess firmly held notions about what features constitute the "best" antibacterial drug targets to interrogate by high-throughput screening of pharmaceutical libraries. We propose that targets with high sequence and/or structural homology to known human drug targets are more likely to find potent inhibitors within the chemical space covered by synthetic pharmaceutical compound libraries and may offer better starting points for novel antibacterial drug discovery efforts.

Additional evidence supporting this approach comes from a recent report in which a small set of ATP-competitive eukaryotic protein kinase inhibitors was screened for inhibition of D-alanine-D-alanine ligase, an essential bacterial enzyme with active-site similarity to eukaryotic protein kinases (18). A subset of these kinase inhibitors exhibited modest inhibition of D-alanine-D-alanine ligase, suggesting that a broader screen of ATP-competitive kinase inhibitor cores might identify additional hits with improved potency.

Like all other clinically useful antibacterial agents, new agents emerging from eukaryotic-like targets must penetrate bacterial cell walls, avoid efflux, and demonstrate selectivity against eukaryotic homologs and/or paralogs. Our internal experience and that of others (2) show that, historically, very few target-based screening hits possess all of these properties, and it is likely that hits identified from screens of eukaryotic-like targets will be no different. The advantage of screening eukaryotic-like targets will come from leveraging the eukaryotic bias of pharmaceutical compound libraries, resulting in more plentiful and potent hits from which to start lead development efforts. A remaining hurdle is our limited understanding of the physicochemical requirements needed to design new inhibitors rationally to penetrate bacterial cell walls and circumvent efflux efficiently. However, several recent reports and reviews describe ongoing, knowledge-based and experimental approaches directed at resolving these fundamental questions (19–21). Finally, the extensive use of lead optimization tools such as structure-based design and computational modeling as described in this article and elsewhere (4) will likely be key for maintaining the bacterial selectivity of the initial hits.

Table 5. In vivo and in vitro pharmacokinetic properties of compound 1

Route and parameters	Rat		Mouse	
Intravenous				
Dose, mg/kg	5		5	
Clearance, mL/min/kg	100		150	
Vd_{ss}, liters/kg	2.2		1.2	
$AUC_{0\to\infty}$, μg/h/mL	0.851		0.558	
$t_{1/2}$, h	1.9		0.22	
Urine recovery, %	3.3		Not collected	
Oral				
Dose, mg/kg	10	200	20	200
C_{max}, μg/mL	0.233	9.19	0.343	27.4
$AUC_{0\to\infty}$, μg/h/mL	0.756	131	0.531	601
F, %	44	>100	24	>100
In vitro				
Human				
Microsomal $t_{1/2}$, min	>60			
Microsomal $clearance_{int}$, μL/min/mg protein	9.63			
Rat				
Microsomal $t_{1/2}$, min				
Microsomal $clearance_{int}$, μL/min/mg protein		5.1 171		
Plasma protein binding, fraction unbound				
Mouse	0.22			
Rat	0.15			
Human	0.14			

Materials and Methods

Macromolecular Synthesis Assay. A sensitized strain of *E. coli* (*tolC imp*) at midlog growth phase was incubated with variable concentrations of compound in the *E. coli* in the presence of radiolabeled precursors [^{14}C]leucine, [^{3}H]thymidine, [^{3}H]uracil, [^{14}C]sodium acetate, or [^{3}H]diaminopimelate for 15 min and then acid-precipitated. The precipitated macromolecules were collected on a filter plate, and the amount of radioactivity incorporated was compared with control to determine an IC_{50}. Further details are provided in *SI Materials and Methods*.

Generation of Mutants Resistant to Pyridopyrimidines. Spontaneously resistant mutants to **1** and **2** were isolated by plating 10^8, 10^9, or 10^{10} cfu of *H. influenzae*, *E. coli*, or *M. catarrhalis* on plates containing compound **1** or **2** in 2-fold increments from 1 to 128 times the agar MIC. After a 48- to 96-h incubation, resistance was confirmed by streaking single colonies on medium containing 2 times the agar MIC of the parent. Selection and propagation of strains are detailed in *SI Materials and Methods*.

Table 6. Antibacterial combination studies with compound 1

Combination agent	Organism (no. of strains)	FIC avg.	Outcome
Azithromycin	*H. influenzae* (4)	0.82–1.23	Additivity
Linezolid	*H. influenzae* (4)	1.05–1.21	Additivity
Ceftazidime	*H. influenzae* (4)	0.84–1.19	Additivity
Ciprofloxacin	*H. influenzae* (1)	0.26	Synergy
Triclosan	*H. influenzae* (1)	0.37	Synergy
Linezolid	Methicillin-resistant *S. aureus* (2)	0.94–1.05	Additivity
Linezolid	*S. pneumoniae* (4)	0.82–1.54	Additivity
Linezolid	*M. catarrhalis* (2)	0.62–0.87	Additivity

Genetic Resistance Mapping in *H. influenzae* and *M. catarrhalis*. To identify region(s) of the *H. influenzae* chromosome harboring mutations responsible for resistance, 10-kb PCR amplicons encompassing the entire genome were generated by using primers described in ref. 22 and a pool of genomic DNA from resistant mutants as template. These amplicons were then used as donor DNAs to transform HI100 in 96-well plates, and cells were plated on plates containing 2, 4, and 8 times the MIC of the parent. These studies identified two overlapping regions of the genome, containing both HI0971 (*accB*) and HI0972 (*accC*), with the ability to move resistance to the parent. To identify the mutation responsible for resistance, the 5-kb overlapping region was PCR-amplified by using individual resistant mutants as template, and the DNA sequence was compared with HI100. Finally, these individual amplicons were used as donor DNAs to create isogenic strains containing the mutation of interest. A similar strategy was used in *M. catarrhalis*; however, amplicons were focused on a region containing *accC* and 1 kb flanking either side.

Determination of Antibacterial Activity. Determination of MICs and MBCs were conducted according to guidelines of the Clinical and Laboratory Standards Institute [CLSI; formerly National Committee on Clinical Laboratory Standards (NCCLS) (23, 24) or according to the procedures described in *SI Materials and Methods*.

Production of Protein Reagents. Standard molecular biology techniques were used to generate protein reagents, and protocols are provided in *SI Materials and Methods*.

Assessment of Inhibitor Binding Thermodynamics by ITC and SPR. Binding of inhibitors to the various BC orthologs was examined by using a VP-ITC (Microcal) and a Biacore S51 SPR instrument (GE Healthcare). Detailed protocols are provided in *SI Materials and Methods*.

ACCase-Coupled Enzyme Assay. A continuous enzyme-coupled phosphate detection assay [based on that of Webb (25) and detailed in Fig. S1] was used to measure the initial rate of the wild-type and mutant *E. coli* ACCase holoenzyme reactions as described in *SI Materials and Methods*.

Protein Crystallization. Crystals of BC with inhibitors were grown at ambient temperature by using the hanging-drop vapor diffusion method. Crystallization drops consisted of equal parts of protein [12 mg/mL, 250 mM potassium chloride, 10 mM Hepes (pH 7.2)] and reservoir solutions consisting of 0.1–0.2 M potassium chloride and 2–4% wt/vol PEG 8000. Before crystallization, the enzyme was incubated with the inhibitors (final concentration, 5 mM) at 4 °C for at least 4 h. The crystals were visible after a few hours and typically grew to dimensions of $0.40 \times 0.40 \times 1.00$ mm. Details of X-ray data collection, structure determination, and refinement are provided in *SI Materials and Methods* and Table S6.

In Vitro Checkerboard Assays. In vitro checkerboard testing was conducted by using 96-well microdilution plates and followed CLSI recommendations for microbroth growth medium, inoculum preparation, and incubation techniques (15). A detailed description of test strains and the protocol used is provided in *SI Materials and Methods*.

Static Time–Kill Assays. In vitro time–kill studies were performed by using 10-mL cultures (initial population of $\approx 5 \times 10^5$ cfu/mL) grown in ambient atmosphere without agitation over a 24-h period. An aliquot of 100 μL was serial-diluted to 10^{-7} in 0.8% saline solution (Baxter) with 10 μL of each sample cultured on chocolate agar (BBL) at selected time intervals according to the method of Miles and Misera (26). Colony-forming units were read after 24-h incubation and reconfirmed after 48-h incubation (100 cfu/mL = limit of detection).

Pharmacokinetic Assessments. Male Sprague–Dawley rats (Charles River Laboratories) were used for rat pharmacokinetic assessments. Animals were housed and maintained in accordance with Pfizer IACUC, State, and Federal guidelines for the humane treatment and care of laboratory animals. All animals were fasted overnight before dosing the next morning, and food was withheld until 4 h after dosing. Water was allowed ad libitum throughout the studies. For each study, blood samples were collected from a carotid artery cannula into EDTA-coated tubes. Sampling occurred at time points up to 7 h after the i.v. and oral dosing of compounds (dosing formulation detailed in *SI Materials and Methods*). Concentrations of compound **1** were determined by a liquid chromatography-tandem MS method after sample preparation by acetonitrile precipitation. Pharmacokinetics calculations were performed by using the noncompartmental approach (linear trapezoidal rule for AUC calculation) with the aid of Watson 6.4 Bioanalytical LIMS (Thermo Electron). Murine pharmacokinetic assessments were similarly conducted by using male CD-1 mice (Charles River Laboratories), except that blood samples were collected by tail vein bleeds over 48 h after oral drug administration.

Murine Infection Models. Animal infection model work was conducted in compliance with National Institutes of Health Guidelines for the Care and Use of Laboratory Animals under a protocol approved by the Pfizer Global Research and Development Animal Use Committee. In vivo efficacy of compound **1** was investigated in a neutropenic murine thigh infection model. Mice (CD-1) were dosed orally with 150 mg/kg and 100 mg/kg cyclophosphamide 4 days and 1 day, respectively, before infection. Typically, 40 mice were infected intramuscularly with 10^7 cfu per animal in 0.1 mL of a 1:1 mixture of Cytodex-1 beads and *H. influenzae* strain HI-3543 (a mouse virulent strain) in *Haemophilus* test medium. Two hours after infection, groups of five mice received oral doses of 400, 200, 100, 50, 25, 12.5, or 0 mg/kg of compound **1** in nanosuspension (see *SI Materials and Methods*). One cohort of mice was killed after inoculation to determine initial bacterial load. Twenty-four hours after inoculation, thighs were removed aseptically and homogenized, and bacterial counts were determined. Efficacy outcome was determined based on recoverable organisms. Plasma samples were also collected at 24 h for analysis of drug concentrations. Details of a *H. influenzae* peritonitis/sepsis model are provided in *SI Materials and Methods*.

ACKNOWLEDGMENTS. We acknowledge the technical contributions and/or scientific advice of the following Pfizer colleagues: Loola Al-Kassim, Fred Boyer, Heather Case, Allison Choy, Phillip Cox, Donna Dunyak, Hongliang Cai, Kelly Fahnoe, Eric Fauman, Jeffery Gage, Michael Herr, Susan Holley, Denton Hoyer, Kristen Kenney, Ji-Young Kim, Karen Leach, Annette Meyer Ruff, Belinda O'Clair, Paul Pagano, Joseph Penzien, Stephen Petras, James F. Smith, Fang Sun, Brenda Vonderwell, Dequing Xiao, and Luping Wu. We also acknowledge the advice and encouragement of Dr. Grover Waldrop.

1. Chan PF, Holmes DJ, Payne DJ (2004) Finding the gems using genomic discovery: Antibacterial drug discovery strategies, the successes and the challenges. *Drug Discov Today* 1:519–527.
2. Payne DJ, Gwynn MN, Holmes DJ, Pompliano DL (2007) Drugs for bad bugs: Confronting the challenges of antibacterial discovery. *Nat Rev Drug Discov* 6:29–40.
3. Pucci MJ (2007) Novel genetic techniques and approaches in the microbial genomics era identification and/or validation of targets for the discovery of new antibacterial agents. *Drugs Res Dev* 8:201–212.
4. Holler TP, Evdokimov AG, Narasimhan L (2007) Structural biology approaches to antibacterial drug discovery. *Exp Opin Drug Dis* 2:1085–1101.
5. Hamby JM, *et al*. (1997) Structure–activity relationships for a novel series of pyrido[2,3-*d*]pyrimidine tyrosine kinase inhibitors. *J Med Chem* 40:2296–2303.
6. Cronan JE, Waldrop GL (2002) Multisubunit acetyl-CoA carboxylases. *Prog Lipid Res* 41:407–435.
7. Bennett LR, Blankley CJ, Fleming RW, Smith RD, Tessman DK (1981) Antihypertensive activity of 6-arylpyrido[2,3-*d*]pyrimidin-7-amine derivatives. *J Med Chem* 24:382–389.
8. Mochalkin IM, *et al*. (2008) Structural evidence for substrate-induced synergism and half-sites reactivity in biotin carboxylase. *Protein Sci* 17:1706–1718.
9. Mohammadi M, *et al*. (1998) Crystal structure of an angiogenesis inhibitor bound to the FGF receptor tyrosine kinase domain. *EMBO J* 17:5896–5904.
10. Dahring TK, *et al*. (1997) Inhibition of growth factor-mediated tyrosine phosphorylation in vascular smooth muscle by PD 089828, a new synthetic protein tyrosine kinase inhibitor. *J Pharmacol Exp Ther* 281:1446–1456.
11. National Committee on Clinical Laboratory Standards (1999) *Methods for Determining Bactericidal Activity of Antibacterial Agents* (National Committee on Clinical Laboratory Standards, Wayne, PA).
12. Amsterdam D (2005) in *Antibiotics in Laboratory Medicine*, ed Lorian V (Lippincott Williams & Wilkins, Philadelphia), pp 61–144.
13. Fernandes P (2006) Antibacterial discovery and development: The failure of success? *Nat Biotechnol* 24:1497–1503.
14. Payne DJ (2008) Desperately seeking new antibiotics. *Science* 321:1644–1645.
15. Pillai SK, Moellering, RC, Eliopoulos, GM (2005) in *Antibiotics in Laboratory Medicine*, ed Lorian V (Lippincott Williams & Wilkins, Philadelphia), pp 365–440.
16. Campbell JW, Cronan JE (2001) Bacterial fatty acid biosynthesis: Targets for antibacterial drug discovery. *Annu Rev Microbiol* 55:305–332.
17. Payne DJ (2004) The potential of bacterial fatty acid biosynthetic enzymes as a source of novel antibacterial agents. *Drug News Perspect* 17:187–194.
18. Triola G, *et al*. (2009) ATP competitive inhibitors of D-alanine-D-alanine ligase based on protein kinase inhibitor scaffolds. *Bioorg Med Chem*, in press.
19. O'Shea R, Moser HE (2008) Physicochemical properties of antibacterial compounds: Implications for drug discovery. *J Med Chem* 22:2871–2878.
20. Multiple authors (2008) Hot topic: Control and regulation of permeability of MDR bacterial pathogens to antibiotics presented by COST Action BM0701. *Curr Drug Targets* 9:718–819.
21. Cai H, Rose K, Liang L-H, Dunham S, Stover C (2009) Development of an LC/MS based drug accumulation assay in Pseudomonas aeruginosa. *Anal Biochem*, in press.
22. Akerley BJ, *et al*. (1998) Systematic identification of essential genes by in vitro mariner mutagenesis. *Proc Natl Acad Sci USA* 95:8927–8932.
23. Clinical Laboratory Standards Institute (2006) *Methods for Dilution Antimicrobial Susceptibility Tests for Bacteria That Grow Aerobically* (Clinical and Laboratory Standards Institute, Wayne, PA), 7th Ed.
24. Clinical Laboratory Standards Institute (2007) *Performance Standards for Antimicrobial Susceptibility Testing* (Clinical and Laboratory Standards Institute, Wayne, PA), 17th Informational Supplement.
25. Webb MR (1992) A continuous spectrophotometric assay for inorganic phosphate and for measuring phosphate release kinetics in biological systems. *Proc Natl Acad Sci USA* 89:4884–4887.
26. Miles AA, Misra SS (1958) The estimation of the bactericidal power of blood. *J Hygiene* 38:732–749.